

Defining the realized niche of the two major clades of *Trichodesmium*: a

2 study on the West Florida Shelf

- 3 Kristina Confesor¹, Corday Selden^{1,2}, Kimberly Powell¹, Laura Donahue³, Travis Mellett^{4,5},
- 4 Salvatore Caprara⁴, Angela N. Knapp⁶, Kristen N. Buck⁴, P. Dreux Chappell¹
- ¹ Old Dominion University, Department of Ocean and Earth Sciences, Norfolk, Virginia, USA
- 6 ² Rutgers University, Department of Marine and Coastal Sciences, New Brunswick, New Jersey,
- 7 USA
- 8 ³ Haverford College, Haverford, Pennsylvania, USA.
- ⁴ University of South Florida, College of Marine Science, St. Petersburg, Florida, USA
- ⁵ University of Washington, School of Oceanography, Seattle, Washington, USA
- ⁶ Florida State University, Department of Earth, Ocean, and Atmospheric Sciences, Tallahassee,
- 12 Florida, USA
- 13 * Correspondence:
- 14 P. Dreux Chappell
- 15 pdchappe@odu.edu
- 16 Keywords: *Trichodesmium*, niche separation, West Florida Shelf, diazotrophs, submarine
- 17 groundwater discharge
- 18 Abstract
- 19 The cyanobacterium *Trichodesmium* plays an essential role supporting ocean productivity by
- 20 relieving nitrogen limitation via dinitrogen (N₂) fixation. The two common *Trichodesmium*
- clades, *T. erythraeum* and *T. thiebautii*, are both observed in waters along the West Florida Shelf
- 22 (WFS). We hypothesized that these taxa occupy distinct realized niches, where *T. thiebautii* is the
- 23 more oceanic clade. Samples for DNA and water chemistry analyses were collected on three separate
- 24 WFS expeditions (2015, 2018, and 2019) spanning multiple seasons; abundances of the single copy
- 25 housekeeping gene *rnpB* from both clades were enumerated via quantitative PCR. We conducted a
- suite of statistical analyses to assess *Trichodesmium* clade abundances in the context of the
- 27 physicochemical data. We observed a consistent coastal vs. open ocean separation of the two
- clades: T. erythraeum was found in shallow waters where the concentrations of dissolved iron (dFe)
- and the groundwater tracer Ba were significantly higher, while *T. thiebautii* abundance was
- 30 positively correlated with water column depth. The Loop Current intrusion in 2015 carrying
- 31 associated entrainment of Missisippi River water brought higher dFe and elevated abundance of both
- 32 clades offshore of the 50 m isobath, suggesting that both clades are subject to Fe limitation on the
- outer shelf. Whereas, previous work has observed that *T. thiebautii* is more abundant than *T.*
- 34 erythraeum in open ocean surface waters, this is the first study to examine Trichodesmium niche
- differentiation in a coastal environment. Understanding the environmental niches of these two key
- 36 taxa bears important implications for their contributions to global nitrogen and carbon cycling and
- their response to global climate change.

1 Introduction

- 39 Trichodesmium is an important genus of marine cyanobacteria that converts dinitrogen gas (N₂) into
- 40 bioaccessible ammonia via N₂ fixation (Capone et al., 2005). Once fixed, new dissolved nitrogen (N)
- 41 can be released, fueling local food webs (Capone, 2001) and, ultimately, playing an essential role in
- 42 total ocean productivity by relieving N limitation (Carpenter and Capone, 2008). Indeed,
- 43 Trichodesmium's new N inputs are estimated at 60-80 Tg N yr (Bergman et al., 2013)—a large
- 44 fraction of the ocean's total estimated N₂ fixation rate of 100-200 Tg N yr⁻¹ (Karl et al., 2002). Thus,
- 45 Trichodesmium's N contributions to the biosphere impacts both the global N and carbon (C) cycles,
- and is thought to influence global carbon dioxide (CO₂) sequestration on hundred-to-thousand-year
- 47 timescales (Gruber and Sarmiento, 1997; Haselkorn and Buikema, 1997; Falkowski, 1998).
- 48 The *Trichodesmium* genus is composed of six different species, grouped into two major clades
- 49 (Hynes et al., 2011; Rouco et al., 2014). Trichodesmium thiebautii and Trichodesmium erythraeum
- are considered the representative species of the two different clades (Rouco et al., 2014), with T.
- 51 thiebautii being the more abundant clade in open ocean regions (Hynes et al., 2011; Chappell et al.,
- 52 2012; Rouco et al., 2014). The groups differ in their ecophysiology, including in their optimal growth
- temperatures and iron (Fe) stress responses (Breitbarth et al., 2007; Chappell and Webb, 2010).
- Nevertheless, most culture-based studies rely on IMS101, a lab strain of *T. erythraeum* first isolated
- off the North Carolina coast roughly 30 years ago (Prufert-Bebout et al., 1993). Work with IMS101
- has suggested that N₂ fixation rates increase commensurately with atmospheric CO₂ (Hutchins et al.,
- 57 2007; Levitan et al., 2007); however, the growth and N₂ fixation responses of *T. thiebautii* and *T.*
- 58 erythraeum differ under rising CO₂ concentrations (Hutchins et al., 2013). Understanding how the
- 59 environmental sensitivities and realized niches of the two clades differ is essential to leveraging
- culture-based work and predicting their response to climate change.
- 61 Trichodesmium is found at tropical latitudes of the ocean (Capone et al., 2005), including along the
- West Florida Shelf (WFS) (Lenes et al., 2001). Surface waters beyond the 50 m isobath offshore of
- Tampa Bay bear low dFe concentrations (Lenes et al., 2001; Mellett and Buck, 2020) that are highly
- 64 influenced by seasonal dust deposition (Mellett and Buck, 2020). Siderophore production in open
- ocean *Trichodesmium* colonies may enable the uptake of dust Fe via siderophore-mediated
- dissolution, making the dust Fe readily available to species with this capability (Basu et al., 2019).
- However, the *T.erythraeum* strain IMS101 is not known to produce siderophores (Basu et al., 2019),
- 68 implying that differences in the capability to produce siderophores in *Trichodesmium* communities
- may lead to niche specialization related to dust deposition.
- Low Fe has been shown to limit both N₂ fixation and growth of *Trichodesmium* (Berman-Frank et al.,
- 71 2001; Kustka et al., 2003). *Trichodesmium* in the open ocean can be co-limited by phosphorus (P)
- and Fe (Mills et al., 2004; Basu et al., 2019), and has been shown to be more strongly P-limited in
- North Atlantic waters in comparison to the North Pacific (Sañudo-Wilhelmy et al., 2001; Sohm et al.,
- North Attailte waters in comparison to the North Lacine (Sando-Willelmy et al., 2001, Solini et al.
- 74 2008). Modeling work has shown that an increase in Fe availability can lead to N₂-fixation by
- 75 Trichodesmium becoming P-limited rather than Fe-limited (Ye et al., 2012). Recently it has been
- found that some *Trichodesmium* species appear to not fix N at all, presumably as a result of
- evolutionary adaptations to resource availability (Delmont, 2021). Little is known about the
- 78 physiology of the non-N₂-fixing *Trichodesmium* species, which have been identified solely through
- metagenomic analysis. Macronutrient concentrations at the WFS are negligible, and well below the
- 80 half-saturation constant for phosphate uptake by *Trichodesmium* (Lenes et al., 2008), suggesting
- 81 these trace macronutrient concentrations are likely to have little impact on clade distribution or
- 82 inhibition of N₂ fixation by nitrate (Knapp et al., 2012).

- 83 Previous work examining clade distributions in the open ocean showed evidence of niche separation
- 84 due to potential resource competition, where *T. thiebautii* distributions extended from the surface
- down to >80 m, while *T. erythraeum* was only observed in the mixed layer of the ocean (Rouco et al.,
- 86 2016). Multiple studies have found that the *T. thiebautii* clade is more abundant than the *T.*
- 87 erythraeum clade in open ocean waters (Hynes et al., 2011; Chappell et al., 2012; Rouco et al., 2014;
- Rouco et al., 2016). Whereas, N₂ fixation rates have been shown to positively correlate with
- 89 dissolved Fe (dFe) concentrations in *T. thiebautii*-dominated open ocean waters (Chappell et al.,
- 90 2012), the niche preferences of the two clades and the environmental controls on their abundance
- 91 remain poorly constrained in coastal areas. Here, we assess the realized niches of the primary
- 92 Trichodesmium clades (T. erythraeum and T. thiebautii) along the WFS by comparing the abundance
- of a housekeeping gene (rnpB) diagnostic of clade identity to physical and chemical variables. By
- 94 elucidating clade-level niche preferences, this work provides insight into the sensitivity of this
- 95 biogeochemically important genus to climate forcings.

2 Methods & Materials

2.1 Hydrographic Data

96

97

108

- 98 Samples were collected on the R/V Weatherbird II from June 18-21 in 2015 and from April 9-12 in
- 99 2019, as well as on the R/V Hogarth from February 27- March 2 in 2018 along the WFS (Figure 1
- and Supplementary Figure 1). Surface salinity and temperature measurements were collected on all
- cruises using the ships' flow-through hydrographic systems (SeaBird). Hydrographic variables such
- as sea surface salinity and sea surface height (SSH) (Figure 1) for the calendar day and region that
- each cruise sampled were obtained using Daily CMEMS GLORYS12V1 global reanalysis (0.083° x
- 104 0.083° resolution) (Lien et al., 2021). SSH was used to outline the edge of the Loop Current for each
- sampling year, while low salinity indicated waters from the Mississippi river were entrained near the
- edge of the Loop Current in each sampling year. Samples for chemical analyses were obtained from
- the surface mixed layer as described below.

2.2 Macronutrient & Trace Metal Analyses

- 109 Surface (~2 m) dFe, barium (Ba), silicic acid (Si) samples were collected using a trace metal clean
- "towfish" system (Mellett and Buck, 2020). The specific sampling system and analytical details for
- trace metal and macronutrient concentration measurements are described in Mellett and Buck
- 112 (Mellett and Buck, 2020). Briefly, trace metal samples were collected with a towfish sampling
- system and in-line filtered through 0.2 µm Acropak capsule filters into acid-cleaned low-density
- polyethylene bottles (dFe and Ba) or polypropylene tubes (Si and PO₄); samples for dissolved trace
- metals were acidified to pH ~1.8 with ultrapure hydrochloric acid (Optima HCl, Fisher; final
- 116 concentration 0.024 M). Macronutrient samples (Si and PO₄, and N+N) were stored frozen (-20 °C)
- until analysis on a Lachat 8500 QuickChem analyzer using colorimetric methods (Parsons et al.,
- 118 1984). Soluble reactive phosphorus (PO₄ or 'phosphate') and nitrate and nitrite ("N+N")
- 119 concentrations were mostly below the detection limit (Supplementary Table 1), which is consistent
- with long term nutrient concentration measurements from the region (Heil et al., 2014). We note that
- the methodology we used for analyzing macronutrients does not incorporate techniques optimized for
- low-level concentration analysis, so PO₄ and N+N were excluded in later statistical
- analyses. Dissolved Fe samples were UV-oxidized, preconcentrated onto a Nobias PA1 chelating
- resin using an automated seaFAST-pico system, and the resulting eluents analyzed using standard
- addition on a Thermo Scientific Element XR Inductively Coupled Plasma Mass Spectrometer in
- medium resolution and counting mode at the University of South Florida (Hollister et al., 2020).

- 127 Dissolved Ba was measured after a 1:50 dilution in 5% ultrapure nitric acid and quantified by
- 128 standard addition within 24 hours of the dilution preparation directly on the Element XR.

129 **DNA Sample Collection**

- 130 Surface DNA samples were collected either via the "towfish" system (Mellett and Buck, 2020) or
- 131 from the ship's Niskin bottle rosette and filtered onto 0.2 µm polyethersulfone (PES) filters using a
- MasterFlex® peristaltic pumping system (AvantorTM, Pennsylvania, USA). Up to 4 L of water was 132
- filtered, with lower volumes of water (1-2 L) collected in 2015. In 2018 and 2019, lower volumes (~1 133
- 134 L) were sometimes collected in the very nearshore waters because of filter clogging. In 2015, flat
- 135 PES filters were stored with Qiagen® RLT Plus buffer (Qiagen, Germany), flash frozen in liquid N₂
- 136 at sea, and then stored at -80 °C until analysis. On the 2018 and 2019 cruises, Sterivex® cartridge
- 137 filters (MilliporeSigma, Burlington, MA) were preserved in RNA later (Life Technologies,
- 138 Carlsbad, CA) at 4 °C for approximately 12-18 hours before being secured in a dry shipper for
- 139 transport and then storage at -80 °C until analysis.

140 2.4 DNA Extraction

- 141 Filters were extracted using the Allprep RNA/DNA Mini Kit (Qiagen, Germany) following the
- 142 manufacturer's protocol with the addition of bead-beating and homogenization using the
- QIAshredder® column (Qiagen, Germany). All extractions were performed in a HEPA filtered UV 143
- 144 sterilized AC600 PCR workstation (AirClean® Systems, Creedmore, NC). For samples collected on
- 145 Sterivex® filters, ethanol cleaned PVC pipe cutters were used to open the Sterivex® tube. The filter
- 146 was then cut out with autoclave-sterilized scalpel blades into two parts, then placed into RLT+ Buffer
- 147 tubes. DNA samples were eluted in 80 µL buffer EB and stored at -80 °C until qPCR analysis.

148 **Quantitative Polymerase Chain Reaction (qPCR)**

- 149 An established qPCR procedure was used for distinguishing between the two primary *Trichodesmium*
- 150 clades (Rouco et al., 2014). Clade-specific primers targeted the single-copy housekeeping gene rnpB,
- which encodes for ribonuclease P and is frequently used in qPCR studies of cyanobacteria (Chappell 151
- 152 and Webb, 2010; Rouco et al., 2014). Quantitative PCR amplification was performed using a Step
- 153 One Plus Real Time PCR thermal cycler (Life Technologies, Carlsbad, CA). The only deviation from
- 154 the original protocol (Chappell and Webb, 2010; Rouco et al., 2014) was that clade-specific gene
- 155 abundances were absolutely quantified using standard curves prepared from T. erythraeum and T.
- 156 thiebautii rnpB plasmids generated and quantified following the protocol of Chappell and Webb (
- 157 2010). All standards, no-template controls, and samples were measured in triplicate with
- 158 PowerSYBR® Green Mastermix fluorescent dye (Life Technologies, Carlsbad, CA) using 96-well
- 159 plates. No-template control wells, used to monitor contamination, contained the qPCR master-mix,
- 160 clade-specific primers, and Rnase-free water. Samples were run as 1:10 dilutions of the original
- 161 extracted DNA with 2 µL of sample in a 20 µL reaction. Melt curves were incorporated to ensure that
- 162 single products were successfully amplified (Rouco et al., 2014) and all qPCR efficiencies were
- 163 above 93%.
- 164 Standard curves were created in triplicate with known gene abundances of serially diluted plasmid
- 165 standards of each clade. The critical threshold, the point at which fluorescence intensity crosses the
- detectible level and corresponds to the initial abundance of DNA in samples (Kralik and Ricchi, 166
- 167 2017), was determined by the Step One Plus software and values from the triplicate qPCR reactions
- 168 for each unknown were averaged and compared with the standard curve. Limits of detection and
- 169 limits of quantification were determined for each sample as described in Selden et al. (2021). In

- subsequent statistical analyses, we chose a conservative approach whereby samples that were below
- detection limit (BDL, < 3 gene copies/PCR) were given the value of zero and samples that were
- detectable but unquantifiable (BQL, <10 gene copies/PCR) were given the value that was the limit of
- detection. Effective limit of quantification (ELOQ) are defined as 2000-3125 copies/L in 2015, 948-
- 174 5000 copies/L in 2018, and 625 2000 copies/L in 2019.

2.6 Statistical Analyses

- Kolmogorov-Smirnov tests were performed to test residuals for normality; however, residuals did not
- follow a normal distribution. Consequently, non-parametric tests (Spearman's Correlation and
- 178 Kruskal-Wallis) using MATLAB, R2020a and ordination statistics (canonical correspondence
- analysis (CCA)) using the VEGAN package in RStudio (Dixon, 2003), were employed to compare
- clade abundances and correlations with environmental data. CCA was done with only one
- 181 constrained axis. Environmental data evaluated for correlation with *Trichodesmium* spp. clades
- included dFe, Si, and Ba concentrations, as well as salinity and water column depth. Water column
- depths were obtained from ETOPO1 (bedrock) bathymetry data grid extraction (Amante and Eakins,
- 184 2009).

186

175

185 3 Results & Discussion

3.1 Physiochemical Data

- On the WFS, surface dFe concentrations were highest near the coast (mean = 3.84 ± 3.14 nM, Table
- 188 1) and declined towards the shelf-break where waters were more oceanic (mean = 0.70 ± 0.62 nM,
- Table 1, Figure 2D-2F, & Supplementary Table 1). Areas near the shelf-break and west of the 50 m
- isobath are defined as offshore, while areas on the mid-shelf with bottom depths <50 m are defined as
- inshore (Figure 2). Concentrations of dFe were negatively correlated with water column depth
- 192 (Spearman: 5.07×10^{-9} , Rho = -0.736). The dFe concentrations were likely elevated in surface waters
- on the shelf due to proximity to continental sources, including riverine and submarine groundwater
- discharge (SGD), and shallow water column mixing with shelf sediments.
- We used Ba and Si to trace continental runoff sources, including inputs from rivers and SGD (Shaw
- et al., 1998; Oehler et al., 2019). Continental runoff can deliver essential nutrients to macro- and
- microbiota living in coastal areas (Charette et al., 2013; Wang et al., 2018), and SGD in particular
- has been previously observed to be important on the inner WFS (<50 m) (Hu et al., 2006). As
- expected, Ba and Si were more abundant at stations with shallower bottom depths (Ba-Spearman:
- 200 1.38x10⁻¹², Rho=-0.817, Si- Spearman: 1.48x10⁻⁸, Rho=-0.711, Table 1) and were also positively
- correlated with one another (Spearman: 3.48x10⁻⁰⁷, Rho=0.659), supporting the hypothesis that
- 202 continental runoff was an important source of these elements on the inner shelf at the time of this
- study.
- Based on salinity and SSH, we collected samples at or near the Loop Current edge on all three
- cruises (Figure 1) (Mellett and Buck, 2020). The Loop Current originates from warm Caribbean
- waters, enters the Gulf of Mexico through the Yucatan Channel and exits via the Florida Strait
- 207 (Morrison et al., 1983). This water mass has been shown to be low in trace metals and
- 208 macronutrients, but serves as a physical vector for bringing elevated dFe concentrations to the outer
- WFS region, by entrainment of Mississippi River plume water along the edge of the Loop that is
- advected south to the WFS (Mellett and Buck, 2020). We observed evidence of this entrainment
- across all three of our cruises (Figure 1 & Figure 2), though the effect on offshore dFe was most
- pronounced in 2018 against the backdrop of much lower wintertime surface dFe (Figure 2E).

213

214

3.2 Trichodesmium Clade Gene Abundance in Coastal vs. Offshore Samples

- Our results support a distinct niche distribution between the two *Trichodesmium* clades along the
- 216 WFS, where *T. erythraeum* dominates the inner shelf (Kruskal-Wallis: p=0.0242, Chisq=5.08, df=66,
- std.dev=200,427) and *T. thiebautii* dominates the outer shelf (Kruskal-Wallis: p=0.000439, Chi-
- sq=12.4, df=66, std.dev=214,000) (Figure 3). Absolute gene abundances of *T. thiebautii* consistently
- averaged between 1.0×10^5 - 1.0×10^6 gene copies/L offshore of the 50 m isobath (Figure 3A-3C),
- comparable with the average cells per L seen in prior studies at further offshore surface waters of the
- Atlantic (Rouco et al., 2014). In many inshore stations, *T. thiebautii* was below detection limits
- (Supplementary Table 1). T. erythraeum, on the other hand, had average ranges of 1.0 x10⁵-1.0 x10⁶
- gene copies/L inshore of the 50 m isobath (Figure 3G-3I). In many offshore stations, *T. erythraeum*
- was not detectable (Supplementary Table 1). Notably, *T. erythraeum* was not detected inshore during
- 225 the 2015 cruise (Figure 3G), but we ascribe this anomaly to a higher detection limit for that specific
- sampling event that precluded quantification (Figure 3G & Supplementary Table 1).

- Altogether, our results support prior studies suggesting that *T. thiebautii* is the more oceanic clade
- (Chappell et al., 2012). It is important to note that on each cruise, stations sampled close to the Loop
- 230 Current had elevated abundances of both *Trichodesmium* clades, which may have contributed to a
- higher mean abundance at offshore stations in 2015 (Figure 3). This may have resulted of the edge of
- the Loop Current delivering dFe and other nutrients to the shelf from entrainment of Mississippi
- 233 River plume water as well as simultaneous dust deposition offshore in this season. The known SGD
- inputs inshore of the 50 m isobath (Hu et al., 2006) may also contribute to the differences in gene
- abundances and perceived environmental niches.
- Before evaluating physicochemical drivers of clade distributions, we focused on water column depth
- as a way to distinguish between inshore and offshore samples. Water column depth and gene
- abundances were compared using multiple non-parametric tests (Spearman correlation and Kruskal-
- Wallis tests) to ensure that results were consistent regardless of analytical tool. Water column depth
- and *T. thiebautii* abundance were positively correlated (Spearman: p=0.0009, Rho=0.4063) while
- bottom depth and *T. erythraeum* abundance were negatively correlated (Spearman: p=0.0123, Rho=-
- 242 0.3114). T. erythraeum was most often observed in waters <50 m depth. Based on these initial
- analyses, we distinguished stations deeper than 50 m as 'offshore' and those shallower as 'inshore'.
- 244 This distinction was used in subsequent statistical analyses. Additionally, prior work has indicated
- 245 that WFS waters <50 m are more influenced by SGD (Hu et al., 2006), which is consistent with the
- elevated dFe and groundwater tracers observed inshore of the 50 m isobath (Figure 2 & 3, Table 1).
- 247 3.3 Gene Abundance Correlations with Physiochemical Data
- To identify potential drivers of niche differentiation between the clades that might explain differences
- between inshore and offshore distributions, we examined correlations between each clade's gene
- abundance with a number of physicochemical variables. Spearman correlations were employed to
- evaluate clade abundances with physiochemical data, while CCA was used to evaluate associations
- between both clades and environmental parameters. Using CCA, significant correlations were found
- between the two clades and dFe and Ba concentrations, as well as water column depth (Figure 4).
- 254 Significant positive correlations were found between salinity and *T. thiebautii* abundance (Spearman
- 255 Correlation (right tail): p= 0.0003, Rho=0.4079), consistent with this being the more oceanic clade as
- salinity increased offshore (Figure 2A-2C). In the CCA analysis, there was no significant correlation

- between the abundance of both clades with salinity; rather, water column depth was significantly
- correlated with the abundance both the clades (Figure 4). This is consistent with *T. thiebautii* being
- 259 the more oceanic clade as water column depth increased, while *T. erythraeum* is the more coastal
- clade associated with shallower water columns.
- Niche differentiation may also be related to ecological competition associated with dFe availability.
- In support of this hypothesis, *T. thiebautii* was negatively correlated with dFe concentration
- 263 (Spearman Correlation, Table 2). CCA, but not Spearman, revealed a correlation between dFe and
- clade abundances (Figure 4), where *T. erythraeum* was positively correlated with dFe, but negative
- 265 correlated with *T. thiebautii*. Prior studies have shown that in Fe-limited open ocean waters, *T.*
- 266 thiebautii is the dominant Trichodesmium clade (Chappell and Webb, 2010); our results suggest that
- 267 when dFe is higher inshore, the oceanic *Trichodesmium* clade representative, *T. thiebautii*, is
- outcompeted by *T. erythraeum*.
- We proffer that this trend is driven by competition with *T. erythraeum* and other phytoplankton
- inshore, meaning that *T. thiebautii* is outcompeted by *T. erythraeum* when dFe from SGD and/or
- other sources is elevated inshore. This is supported by the observations that *T. thiebautii* was also
- 272 negatively correlated with Ba and Si concentrations (Spearman Correlation, Table 2), while dFe and
- Ba were positively correlated with *T. erythraeum* (CCA, Figure 4), in particular during the Loop
- 274 Current intrusion in 2015. The Loop Current intrusion resulted in enhanced offshore *T. erythraeum*
- abundance in 2015 (Fig 3G and Supplementary Table 1). However, we do not see *T. erythraeum*
- abundance elevated offshore in 2018 (Figure 3E and Supplementary Table 1), even though there was
- elevated dFe offshore as a result of the Loop Current intrusion (Figure 2E, Supplementary Table 1).
- This suggests that *T. erythraeum* is also Fe-limited offshore of the 50 m isobath on the WFS,
- potentially due to the lack of siderophore production mechanisms that open ocean *Trichodesmium*
- colonies have (Basu et al., 2019), except in situations where entrainment of dFe from continental
- runoff sources is carried by Loop Current to offshore locations.

282 4 Conclusion

- Our findings show that the two main *Trichodesmium* clades, *T. thiebautii* and *T. erythraeum*, occupy
- distinct realized niches on the WFS. T. thiebautii is the more oceanic clade: its abundance was
- elevated in samples collected at deeper stations (>50 m), with elevated salinity and lower dFe. T.
- 286 erythraeum is more coastal: it was most abundant at shallow stations with significant continental
- runoff inputs and higher dFe, and appears to outcompete *T. thiebautii* in coastal regions. These
- distinct niche occupations are likely due to resource competition between the two clades at stations
- with higher dFe. More work is needed to identify the metabolic pathways that distinguish the two
- clades and lead to the observed distinctions in distribution patterns. The intrusion of the Loop Current
- and associated entrainment of Missisippi River water brought higher dFe and elevates gene
- abundances of the two clades offshore of the 50 m isobath, suggesting that both clades are subject to
- Fe limitation on the outer shelf. Understanding the environmental niches of these two key taxa bears
- important implications for their contributions to global N and C cycling and their response to global
- 295 climate change.

5 Conflict of Interest

- 297 The authors declare that the research was conducted in the absence of any commercial or financial
- relationships that could be construed as a potential conflict of interest.

300 6 Author Contributions

- ANK, KNB, and PDC designed the sampling program. CS, KC, and PDC designed the
- 302 Trichodesmium analysis plan. All authors were involved in sample collection and/or analysis. KC,
- 303 CS, and PDC wrote the initial manuscript draft. All other authors contributed to manuscript editing
- and approved the final manuscript.

305 7 Funding

- Funding for this study was provided by Old Dominion University, the Jeffress Trust Awards Program
- in Interdisciplinary Research, a FSU Planning Grant (ANK), the National Science Foundation
- 308 through the Research Experience for Undergraduates Program (PDC), and subsidized ship-time from
- the Florida Institute of Oceanography to KNB.

310 8 Acknowledgments

- We thank the Captain and crews of the R/V Weatherbird II and R/V Hogarth. We also thank Zuzanna
- 312 Abdala for assistance with sample collection in 2015, and Sveinn Einarsson for assistance with
- 313 Python coding. We thank Chelsea Bonnain Chase, Eric Rabinowitz, and Adrienne Hollister for their
- 314 help with field sampling, and Gabe Browning for analyzing Ba in a subset of these samples.

315 9 Data Availability Statement

- The datasets analyzed for this study is available for direct download (Supplementary Table 1) and are
- archived in the Biological and Chemical Oceanography Data Management Office (https://www.bco-
- 318 dmo.org/project/814733).

319 10 Figure Captions

- Figure 1. WFS study region for June 2015 (1A), February-March 2018 (1B), and April 2019 (1C).
- 321 Overlying sea surface salinity (note different color scales for each panel) from GLORYS12V1 (Lien
- et al., 2021). White dots indicate stations. Dashed, dotted, and solid lines indicate a SSH of 0 m, 0.2
- m, and 0.4 m respectively, outlining the edge of the Loop Current.
- Figure 2. Salinity (2A-2C) and dFe concentration (2D-2F) measurements from each sampling year
- plotted over bathymetry extracted from ETOPO1 bedrock (Amante and Eakins, 2009). Dashed line
- indicates the 50 m isobath which is used to distinguish between offshore and inshore samples and
- indicates where there are known SGD inputs inshore of this area (Hu et al., 2006).
- Figure 3. Absolute gene abundance for *T. thiebautii* (3A-3C) and *T. erythraeum* (3G-3I), as well as
- relative gene abundance for *T. thiebautii* (3D-3F) and *T. erythraeum* (3J-3L) with contours reflecting
- bathymetry extracted from ETOPO1 bedrock (Amante and Eakins, 2009). In all panels, the dashed
- line indicates the 50 m isobath, which is used to distinguish between offshore and inshore samples
- and indicates where there are known SGD inputs inshore of this area (Hu et al., 2006). Triangles
- represent *Trichodesmium* spp. abundances below the detection limit (BDL), while squares represent
- data that is below the quantification limit (BQL). (Effective limit of quantification (ELOQ): 2000-
- 335 3125 copies/L in 2015, 948-5000 copies/L in 2018, and 625 2000 copies/L in 2019).
- Figure 4. CCA model of gene abundances of both clades in relation to physiochemical data and
- water column depth (extracted from ETOPO1 bedrock (Amante and Eakins, 2009). Clades are

- labeled on the data points, while blue arrows show the x-axis directionality of physiochemical data and environmental parameters. There was only one constrained axis as there were only two clades of interest. Significant environmental parameters and the two clades included dFe (nM) (p-value= 0.001 Chi-square=0.116). Water column depth (m) (p-value=0.001 Chi-square=0.058), and Ba (nM)
- 341 0.001, Chi-square=0.116), Water column depth (m) (p-value=0.001, Chi-square=0.058), and Ba (nM) (p-value=0.001, Chi-square=0.490).
- Supplementary Figure 1. WFS study region for June 2015 (1A), February-March 2018 (1B), and April 2019 (1C). Gray lines represent cruise track.

11 Tables

345

350

351

352

353

354

355

356

357

358

359

360

361

Table 1. Average values and standard deviations of physiochemical data from 2019 (first two columns) and from all three cruises combined (last two columns). Values from 2015 & 2018 are reported in Mellet and Buck (2020). Offshore is defined as west of the 50 m isobath, and inshore as all measurements east of the 50 m isobath.

Measurement	Offshore 2019	Inshore 2019	Offshore Total	Inshore Total
dFe (nM)	0.400 ± 0.15	2.81 ± 1.50	0.70 ± 0.62	3.84 ± 3.14
Ba (nM)	46.2 ± 5.7	59.1 ± 7.0	48.9 ± 3.8	61.1 ± 9.7
Si (uM)	1.07 ± 0.20	2.02 ± 1.08	0.95 ± 0.65	2.31 ± 1.76
Salinity	36.4 ± 0.1	35.0 ± 0.8	36.5 ± 0.2	35.4 ± 0.9

Table 2. Spearman individual correlations between *Trichodesmium* clades and chemical concentrations. Asterisks indicate a significant p-value.

364

362

363

Element concentration correlations	p-value	Rho
dFe & T. thiebautii (left-tail)*	0.0047	-0.3794
Ba & T. thiebautii (left-tail)*	0.0133	-0.3201
Si & T. thiebautii (left-tail)*	0.0082	-0.3446
Salinity & T. thiebautii (right-tail)*	0.000149	0.4284
Water Column Depth & T. thiebautii (right-tail)*	0.0000302	0.4698
dFe & T. erythraeum (right-tail)	0.368	0.0511
Ba & T. erythraeum (right-tail)*	0.0172	0.3059
Si & T. erythraeum (right-tail)	0.113	0.1779
Salinity & T. erythraeum (left-tail)	0.1486	-0.1293
Water Column Depth & T. erythraeum (left-tail)*	0.0200	-0.2516

12 References

365

369

370

371

Amante C, Eakins B W (2009). ETOPO1 1 Arc-Minute Global Relief Model: Procedures, Data
 Sources and Analysis. NOAA Technical Memorandum NMFS F/SPO: National Marine
 Fisheries Service, NOAA

Basu S, Gledhill M, De Beer D, Prabhu Matondkar S G, Shaked Y (2019). Colonies of marine cyanobacteria *Trichodesmium* interact with associated bacteria to acquire iron from dust. Communications Biology, 2(1): 284

- Bergman B, Sandh G, Lin S, Larsson J, Carpenter E J (2013). *Trichodesmium* a widespread marine cyanobacterium with unusual nitrogen fixation properties. FEMS Microbiology Reviews, 37(3): 286-302
- Berman-Frank I, Cullen J T, Shaked Y, Sherrell R M, Falkowski P G (2001). Iron availability,
 cellular iron quotas, and nitrogen fixation in *Trichodesmium*. Limnology and Oceanography,
 46(6): 1249-1260
- Breitbarth E, Oschlies A, Laroche J (2007). Physiological constraints on the global distribution of *Trichodesmium* – effect of temperature on diazotrophy. Biogeosciences, 4(1): 53-61

- Capone D G (2001). Marine nitrogen fixation: what's the fuss? Current Opinion in Microbiology, 4(3): 341-348
- Capone D G, Burns J A, Montoya J P, Subramaniam A, Mahaffey C, Gunderson T, Michaels A F,
 Carpenter E J (2005). Nitrogen fixation by *Trichodesmium spp.*: An important source of new
- nitrogen to the tropical and subtropical North Atlantic Ocean. Global Biogeochemical Cycles, 19(2)
- Carpenter E J, Capone D G (2008). Nitrogen Fixation in the Marine Environment: Elsevier, 141-198
- Chappell P D, Moffett J W, Hynes A M, Webb E A (2012). Molecular evidence of iron limitation and availability in the global diazotroph *Trichodesmium*. The ISME journal, 6(9): 1728-1739
- Chappell P D, Webb E A (2010). A molecular assessment of the iron stress response in the two phylogenetic clades of *Trichodesmium*. Environmental Microbiology, 12(1): 13-27
- Charette M A, Henderson P B, Breier C F, Liu Q (2013). Submarine groundwater discharge in a river-dominated Florida estuary. Marine Chemistry, 156: 3-17
- Delmont T O (2021). Discovery of nondiazotrophic *Trichodesmium*; species abundant and widespread in the open ocean. Proceedings of the National Academy of Sciences, 118(46): e2112355118
- Dixon P (2003). VEGAN, a package of R functions for community ecology. Journal of Vegetation
 Science, 14(6): 927-930
- Falkowski P G (1998). The Oceanic Photosynthetic Engine: Origins, Evolution, and Role in Global Biogeochemical Cycles: Springer Netherlands, 3941-3947
- Gruber N, Sarmiento J L (1997). Global patterns of marine nitrogen fixation and denitrification.
 Global Biogeochemical Cycles, 11(2): 235-266
- Haselkorn R, Buikema W J (1997). Heterocyst Differentiation and Nitrogen Fixation in
 Cyanobacteria: Springer Berlin Heidelberg, 163-166
- Heil C A, Dixon L K, Hall E, Garrett M, Lenes J M, O'neil J M, Walsh B M, Bronk D A, Killberg Thoreson L, Hitchcock G L, Meyer K A, Mulholland M R, Procise L, Kirkpatrick G J, Walsh
 J J, Weisberg R W (2014). Blooms of *Karenia brevis* on the West Florida Shelf: Nutrient
 sources and potential management strategies based on a multi-year regional study. Harmful
 Algae, 38: 127-140
- Hollister A P, Kerr M, Malki K, Muhlbach E, Robert M, Tilney C L, Breitbart M, Hubbard K A,
 Buck K N (2020). Regeneration of macronutrients and trace metals during phytoplankton
 decay: An experimental study. Limnology and Oceanography, 65(8): 1936-1960
- Hu C, Muller-Karger F E, Swarzenski P W (2006). Hurricanes, submarine groundwater discharge, and Florida's red tides. Geophysical Research Letters, 33(11)
- Hutchins D A, Fu F-X, Webb E A, Walworth N, Tagliabue A (2013). Taxon-specific response of marine nitrogen fixers to elevated carbon dioxide concentrations. Nature Geoscience, 6(9): 790-795
- Hutchins D A, Fu F X, Zhang Y, Warner M E, Feng Y, Portune K, Bernhardt P W, Mulholland M R
 (2007). CO2 control of *Trichodesmium* N₂ fixation, photosynthesis, growth rates, and
- elemental ratios: Implications for past, present, and future ocean biogeochemistry. Limnology and Oceanography, 52(4): 1293-1304

- 421 Hynes A M, Webb E A, Doney S C, Waterbury J B (2011). Comparison of cultured *Trichodesmium*
- 422 (Cyanophyceae) with species characterized from the field. Journal of Phycology, 48(1): 196-
- 423 210
- Karl D, Michaels A, Bergman B, Capone D, Carpenter E, Letelier R, Lipschultz F, Paerl H, Sigman
 D, Stal L (2002). Dinitrogen fixation in the world's oceans. Biogeochemistry, 57(1): 47-98
- 426 Knapp A N, Dekaezemacker J, Bonnet S, Sohm J A, Capone D G (2012). Sensitivity of
- 427 Trichodesmium erythraeum and Crocosphaera watsonii abundance and N2 fixation rates to
- varying NOU and PO43 concentrations in batch cultures. Aquatic Microbial Ecology, 66:
- 429 223-236
- Kralik P, Ricchi M (2017). A Basic Guide to Real Time PCR in Microbial Diagnostics: Definitions,
 Parameters, and Everything. Frontiers in microbiology, 8: 108-108
- Kustka A B, Sañudo-Wilhelmy S A, Carpenter E J, Capone D, Burns J, Sunda W G (2003). Iron
- requirements for dinitrogen- and ammonium-supported growth in cultures of *Trichodesmium*
- 434 (IMS 101): Comparison with nitrogen fixation rates and iron: carbon ratios of field
- populations. Limnology and Oceanography, 48(5): 1869-1884
- Lenes J M, Darrow B A, Walsh J J, Prospero J M, He R, Weisberg R H, Vargo G A, Heil C A
- 437 (2008). Saharan dust and phosphatic fidelity: A three-dimensional biogeochemical model of
- 438 *Trichodesmium* as a nutrient source for red tides on the West Florida Shelf. Continental Shelf
- 439 Research, 28(9): 1091-1115
- Lenes J M, Darrow B P, Cattrall C, Heil C A, Callahan M, Vargo G A, Byrne R H, Prospero J M,
- Bates D E, Fanning K A, Walsh J J (2001). Iron fertilization and the *Trichodesmium* response on the West Florida shelf. Limnology and Oceanography, 46(6): 1261-1277
- Levitan O, Rosenberg G, Setlik I, Setlikova E, Grigel J, Klepetar J, Prasil O, Berman-Frank I (2007).
- Elevated CO2 enhances nitrogen fixation and growth in the marine cyanobacterium
- 445 Trichodesmium. Global Change Biology, 13(2): 531-538
- Lien V S, Øie Nilsen J E, Perivoliotis L, Sotiropoulou M, Denaxa D, Ehrhart S, Seppälä J, Racapé V
- 447 (2021). BioGeoChemical product provided by the Copernicus Marine Service: Copernicus
- 448 GmbH
- Mellett T, Buck K N (2020). Spatial and temporal variability of trace metals (Fe, Cu, Mn, Zn, Co, Ni,
- Cd, Pb), iron and copper speciation, and electroactive Fe-binding humic substances in surface
- waters of the eastern Gulf of Mexico. Marine Chemistry, 227: 103891
- 452 Mills M, Ridame C, Davey M, Laroche J, Geider R (2004). Mills MM, Ridame C, Davey M, La
- Roche J, Gelder RJ.. Iron and phosphorus co-limit nitrogen fixation in the eastern tropical
- North Atlantic. Nature 429: 292-294. Nature, 429: 292-294
- 455 Morrison J M, Merrell W J, Key R M, Key T C (1983). Property distributions and deep chemical
- measurements within the western Gulf of Mexico. Journal of Geophysical Research, 88(C4):
- 457 2601
- Oehler T, Tamborski J, Rahman S, Moosdorf N, Ahrens J, Mori C, Neuholz R, Schnetger B, Beck M
- 459 (2019). DSi as a Tracer for Submarine Groundwater Discharge. Frontiers in Marine Science,
- 460 6
- Parsons T R, Maita Y, Lalli C M (1984). A Manual of Chemical & Biological Methods for Seawater
- Analysis. Parsons, T.R., Maita, Y. and Lalli, C.M. (eds). Amsterdam: Pergamon, xiii-xiv

463 464 465	Prufert-Bebout L, Paerl H, Lassen C (1993). Prufert-Bebout L, Paerl HW, Lassen C Growth, nitrogen fixation, and spectral attenuation in cultivated <i>Trichodesmium</i> species. Appl Environ Microbiol 59: 1367-1375. Applied and environmental microbiology, 59: 1367-1375
466 467 468	Rouco M, Haley S T, Alexander H, Wilson S T, Karl D M, Dyhrman S T (2016). Variable depth distribution of <i>Trichodesmium</i> clades in the North Pacific Ocean. Environmental Microbiology Reports, 8(6): 1058-1066
469 470 471	Rouco M, Warren H J, Mcgillicuddy D J, Waterbury J B, Dyhrman S T (2014). <i>Trichodesmium sp.</i> clade distributions in the western North Atlantic Ocean. Limnology and Oceanography, 59(6): 1899-1909
472 473 474	Sañudo-Wilhelmy S A, Kustka A B, Gobler C J, Hutchins D A, Yang M, Lwiza K, Burns J, Capone D G, Raven J A, Carpenter E J (2001). Phosphorus limitation of nitrogen fixation by <i>Trichodesmium</i> in the central Atlantic Ocean. Nature, 411(6833): 66-69
475 476 477 478	Selden C R, Chappell P D, Clayton S, Macías-Tapia A, Bernhardt P W, Mulholland M R (2021). A coastal N ₂ fixation hotspot at the Cape Hatteras front: Elucidating spatial heterogeneity in diazotroph activity via supervised machine learning. Limnology and Oceanography, 66(5): 1832-1849
479 480 481	Shaw T J, Moore W S, Kloepfer J, Sochaski M A (1998). The flux of barium to the coastal waters of the southeastern USA: the importance of submarine groundwater discharge. Geochimica et Cosmochimica Acta, 62(18): 3047-3054
482 483 484	Sohm J A, Mahaffey C, Capone D G (2008). Assessment of relative phosphorus limitation of <i>Trichodesmium spp</i> . in the North Pacific, North Atlantic, and the north coast of Australia. Limnology and Oceanography, 53(6): 2495-2502
485 486 487	Wang X, Li H, Zheng C, Yang J, Zhang Y, Zhang M, Qi Z, Xiao K, Zhang X (2018). Submarine groundwater discharge as an important nutrient source influencing nutrient structure in coastal water of Daya Bay, China. Geochimica et Cosmochimica Acta, 225: 52-65
488 489 490	Ye Y, Völker C, Bracher A, Taylor B, Wolf-Gladrow D A (2012). Environmental controls on N ₂ fixation by <i>Trichodesmium</i> in the tropical eastern North Atlantic Ocean—A model-based study. Deep Sea Research Part I: Oceanographic Research Papers, 64: 104-117
491	
492	

Figure 1. WFS study region for June 2015 (1A), February-March 2018 (1B), and April 2019 (1C). Overlying sea surface salinity (note different color scales for each panel) from GLORYS12V1 (Lien et al., 2021). White dots indicate stations. Dashed, dotted, and solid lines indicate a SSH of 0 m, 0.2 m, and 0.4 m respectively, outlining the edge of the Loop Current.

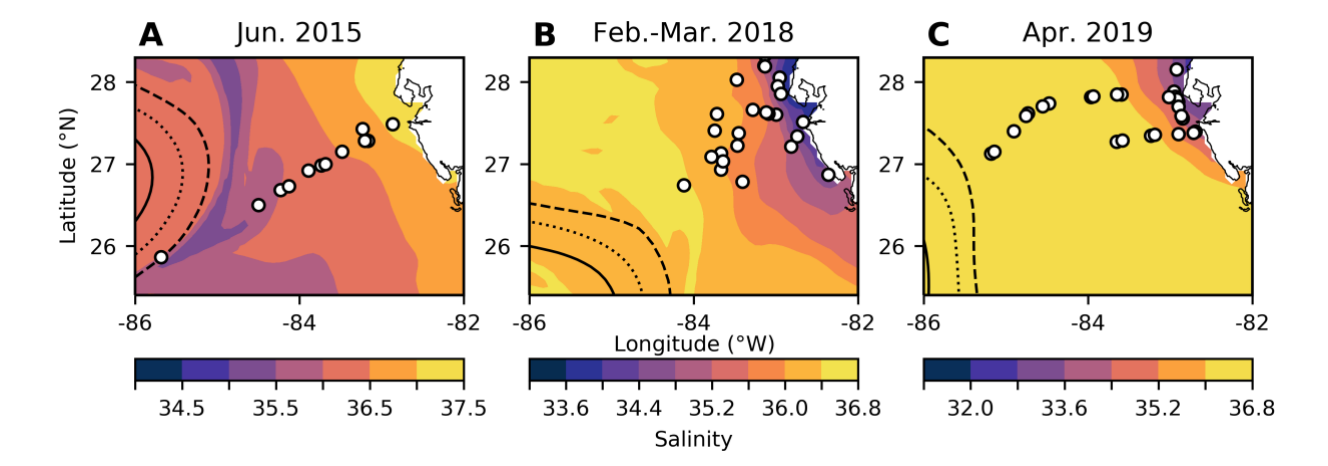


Figure 2. Salinity (2A-2C) and dFe concentration (2D-2F) measurements from each sampling year plotted over bathymetry extracted from ETOPO1 bedrock (Amante and Eakins, 2009). Dashed line indicates the 50 m isobath which is used to distinguish between offshore and inshore samples and indicates where there are known SGD inputs inshore of this area (Hu et al., 2006).

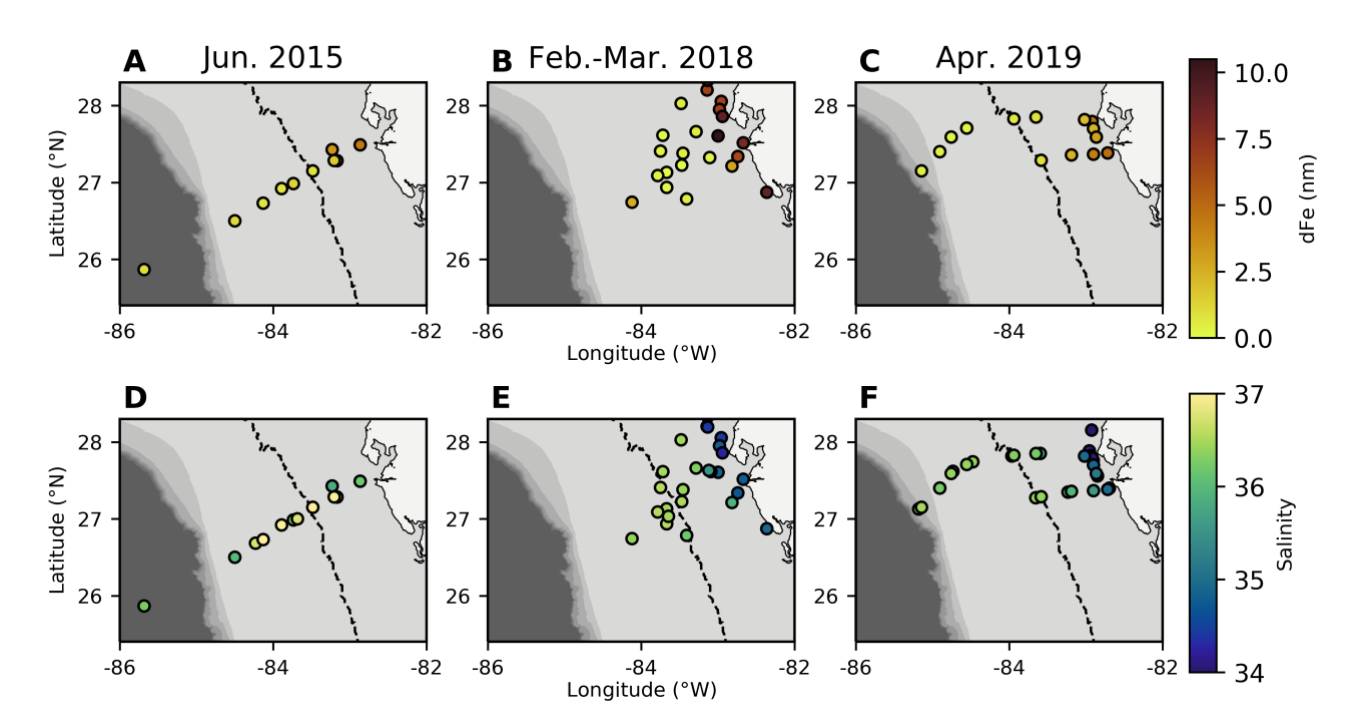


Figure 3. Absolute gene abundance for *T. thiebautii* (3A-3C) and *T. erythraeum* (3G-3I), as well as relative gene abundance for *T. thiebautii* (3D-3F) and *T. erythraeum* (3J-3L) with contours reflecting bathymetry extracted from ETOPO1 bedrock (Amante and Eakins, 2009). In all panels, the dashed line indicates the 50 m isobath, which is used to distinguish between offshore and inshore samples and indicates where there are known SGD inputs inshore of this area (Hu et al., 2006). Triangles represent *Trichodesmium* spp. abundances below the detection limit (BDL), while squares represent data that is below the quantification limit (BQL). (Effective limit of quantification (ELOQ): 2000-3125 copies/L in 2015, 948-5000 copies/L in 2018, and 625 – 2000 copies/L in 2019).

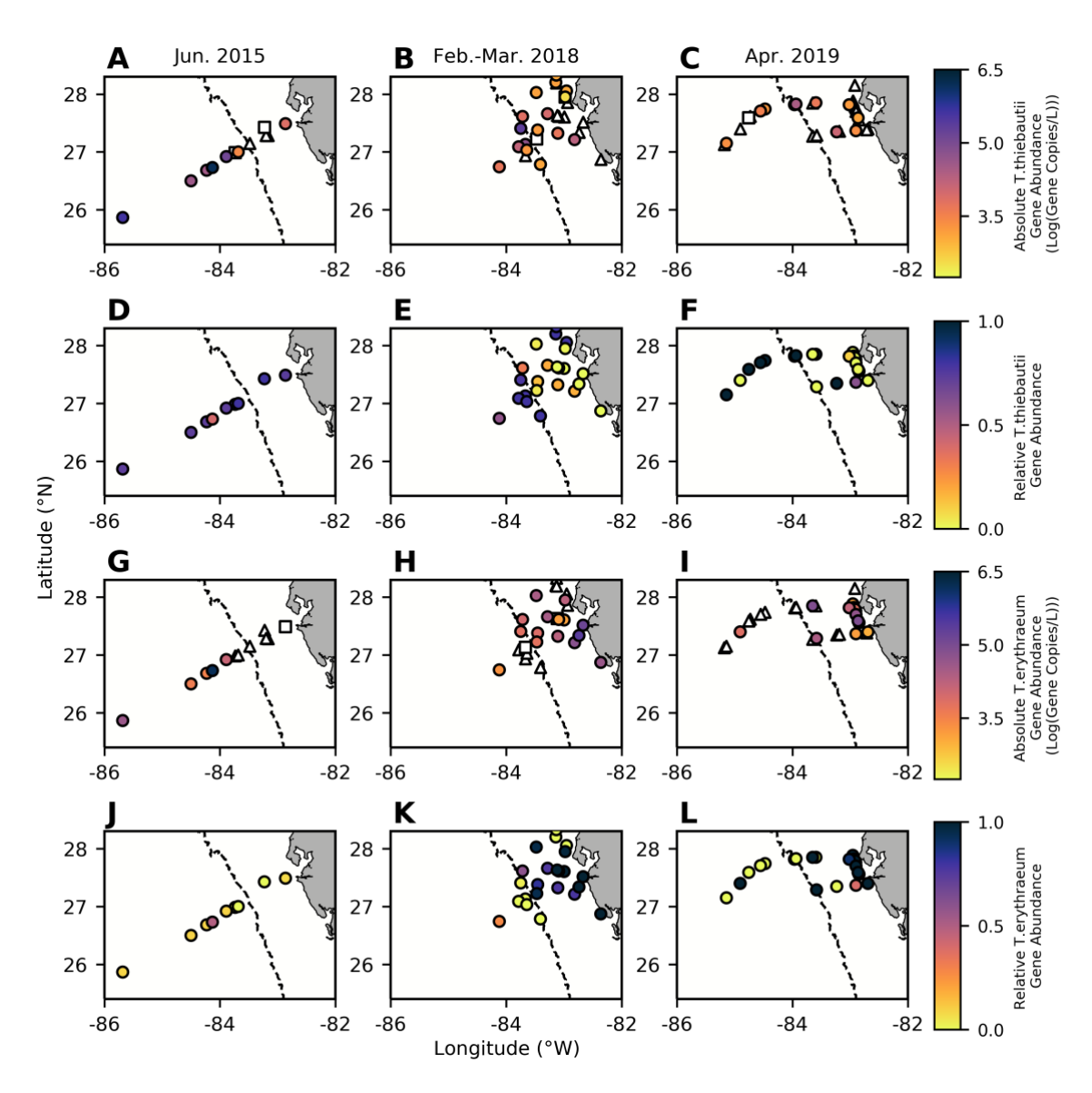


Figure 4. CCA model of gene abundances of both clades in relation to physiochemical data and water column depth (extracted from ETOPO1 bedrock (Amante and Eakins, 2009). Clades are labeled on the data points, while blue arrows show the x-axis directionality of physiochemical data and environmental parameters. There was only one constrained axis as there were only two clades of interest. Significant environmental parameters and the two clades included dFe (nM) (p-value= 0.001, Chi-square=0.116), Water column depth (m) (p-value=0.001, Chi-square=0.058), and Ba (nM) (p-value=0.001, Chi-square=0.490).

